Int. j. adv. multidisc. res. stud. 2023; 3(5):651-654

Received: 09-08-2023
Accepted: 19-09-2023

International Journal of Advanced Multidisciplinary Research and Studies

ISSN: 2583-049X

Bone CT Radiomics is Feasible in Identifying CKD5

[1] Hissein Mahamat Fadoul, [2] Xiaoming Li, [3] Gang Wu, [4] MD Yongli Yang, [5] MD Donglin Wen

[1, 2, 3, 5] Department of Radiology, Tongji Hospital, Tongji Medical College of Huazhong University of Science and Technology, Wuhan, China

[4] Department of Radiology, Hubei No. 3 People's Hospital of Jianghan University, Wuhan, China

Corresponding Author: **Xiaoming Li, Gang Wu**

Abstract

Introduction: We aimed to investigate the feasibility of bone CT radiomics in identifying CKD5. 120 chronic kidney disease (CKD) patients (60 CKD5 and 60 CKD1) were assessed using the bone CT radiomics method. Radiomics features of the vertebral CT images were obtained by using 3D Slicer software, and then were compared between CKD5 and CKD1 cases. Logic regression model was used for the features with significance. The receiver operating characteristic (ROC) curve was used to determine the performance in identifying CKD5. Mean CT density was not significantly different between the two groups (P=0.12). CKD1 and CKD5 cases differed in the following features: Contrast, Correlation, Dependence Variance, and Dependence Entropy (P<0.05). The AUC of the regression model was 0.854.

The sensitivity and specificity of the model in identifying CKD5 were 88% (53/60) and 87% (52/60) respectively.

Conclusion: Bone CT radiomics is feasible in identifying CKD5.

Keywords: Bone, CT Radiomics, Chronic Kidney Disease, CKD5

Introduction

Chronic kidney disease (CKD) is a common disease that affected millions of people in the world [1]. Reduced blood calcium and elevated blood phosphorus in CKD may cause secondary hyperparathyroidism or bone metabolism disorder [2, 3]. Renal Osteodystrophy (ROD) is a common complication of end-stage renal disease [4]. Fibrous osteoarthritis was observed in some CKD cases, demonstrating as local destruction of bone structure. Bone loss and strength decrease were more frequently seen in CKD, increasing the risk of fracture [5]. Bone mineral density (BMD) test is useful for diagnosing osteoporosis [6, 7], but is not routinely used for CKD patients. Compared to BMD test, CT examination is more frequently used to detect osteoporosis and fibrous osteoarthritis [8]. Bone mass and fat content can influence bone CT attenuation value [9, 10]. As bone mass and fat content both vary with age, bone CT attenuation also changes with time. Young and old people differed in bone CT attenuation. As CT attenuation is influenced by fat content and age, it is seldom used for the evaluation of osteoporosis [11, 12]. The data regarding normal range of bone CT attenuation in each age is still lacking. CT attenuation is thus not feasible for the discrimination of CKD patients and normal people. Other CT parameters are urgently required for the CKD evaluation, which should avoid the influence of fat content and age.

In recent years, CT radiomics has been applied to many diseases, significantly improving diagnostic accuracy [13-18]. Some radiomics features besides CT attenuation were found significantly different between two categories, so can be used for the discrimination. Logic regression model can be established using the significant features. The regression model generally provides higher diagnostic accuracy than any single feature. There are many publications reporting the value of CT radiomics in the discrimination of bone diseases [19- 21]. However, to the best of the authors' knowledge, there is no study using bone CT radiomics to evaluate bone microstructure change caused by CKD. The purpose of the study is thus to investigate the feasibility of bone CT radiomics in identifying CKD5.

Materials and Methods

This is a retrospective study approved by the Institutional Review Broad of the university. Informed consent was obtained from patients before the study. The inclusion criteria for CKD5 patients were: glomerular filtration rate (GFR)<15ml/min and non-contrast enhanced CT of the L1 vertebra. The inclusion criteria for CKD1 patients were: GFR≥90ml/min and non-contrast

enhanced CT of the L1 vertebra. In the study, CKD1 and CKD5 patients were strictly paired. Each pair of CKD1 and CKD5 had the same age and gender. Patients that were not paired were excluded from the study. In the study, 60 CKD1 cases and 60 CKD5 patients matched in age and gender, and were analyzed by using radiomics method.

Radiomic Feature Extraction

The source data of non-contrast-enhanced CT were transferred to a dedicated workstation with the software of 3D-slicer (version 4.11). The radiomics features of L1 vertebral image were extracted by two radiologists with 7 and 6 years of experience in diagnosing skeletal diseases. They were blinded to the patient's age, gender, and CKD stage. An oval or circle ROI was drawn on the transverse section of the L1 vertebra. The diameter of the ROI was asked to be slightly less than that of the vertebra. The ROI should not be placed on the slices near the end plate. Radiomics features of the ROI were extracted with the function tool of radiomics. In the study, the following feature classes were chosen: first order, glcm, gldm, glrlm, glszm, and ngtdm. A total of 93 features were obtained for each ROI in the study.

Statistical Analysis

All statistical analysis was performed with SPSS. Intra-class correlation coefficient (ICC) was calculated to determine inter-reader reproducibility in the measurement of radiomics features. Features with ICC＞0.7 were compared between the two groups. We assessed differences between CKD1 and CKD5 cases using the two-sample t-test for normal distribution data or the Mann-Whitney U test for non-normal continuous variables. Features with P values less than 0.05 were considered significant features, which were used in the Logic regression model. The receiver operator characteristic (ROC) curve was constructed for determining the area under the curve (AUC). The Z test was used to compare AUC values.

Results

From September 2017 to May 2022, 60 CKD1 cases and 60 CKD5 cases with non-contrast-enhanced CT of the L1 vertebra were analyzed in the study. 93 radiomics features of vertebra images were successfully extracted. CKD patients' ages range from 31 to 73 years, with a median of 52. 64 out of 120 patients were female.

The GFR of CKD1 cases ranged from 92.4 ml/min to 99.3 ml/min, with an average of 95.8 ml/min. The main accompanied diseases of the CKD1 cohort were as follows: chronic nephritis (n=41), diabetes (n=11), hypertension (n=24), gout (n=9); chronic respiratory disease (n=7), chronic cardiovascular disease (n=6), tumor (n=2), tuberculosis (n=2). The body mass index (BMI) of CKD1 patients ranged from 16.7 to 26.1, with an average of 21.2.

The GFR of CKD5 cases ranged from 6.4 ml/min to 13.3 ml/min, with an average of 9.8 ml/min. The main accompanied diseases of the CKD5 cohort were as follows: chronic nephritis (n=60), diabetes (n=17), hypertension (n=33), gout (n=15); chronic respiratory disease (n=12), chronic cardiovascular disease (n=9), tumor (n=4), tuberculosis (n=3). The BMI of CKD5 patients ranged from 14.5 to 24.1, with an average of 18.9.

Mean (grayscale) is one of the first-order features, equal to average of CT density. In the study, mean CT density of bone was slightly higher in CKD1versus CKD5, but the difference did not reach statistical significance (165.4±87.2 vs. 144.2±67.4, P=0.12).

CKD1 and CKD5 bones differed in the following four features (P<0.05, Table 1):

Table 1: The bone CT radiomics features were compared between CKD1 and CKD5 cases

	CKD5	CKD1	P value
Mean	144.2±67.4	165.4±87.2	0.12
Contrast	4.85±1.21	2.15±0.76	0.02
Correlation	0.35±0.14	0.57±0.19	0.021
Dependence Variance	1.95±0.24	1.73±0.19	0.024
Dependence Entropy	4.95±1.24	5.23±1.36	0.037

Contrast, Correlation, DependenceVariance, and DependenceEntropy. Contrast was significantly higher in CKD5 versus CKD1 (4.85±1.21 vs. 2.15±0.76, P=0.02). Correlation was significantly lower in CKD5 (0.35±0.14 vs. 0.57±0.19, P=0.021). DependenceVariance was significantly higher in CKD5 (1.95±0.24 vs. 1.73±0.19, P=0.024). DependenceEntropy was significantly lower in CKD5 (4.95±1.24 vs. 5.23±1.36, P=0.037). AUC ranged from 0.635 to 0.789 for the four features (see Fig 1).

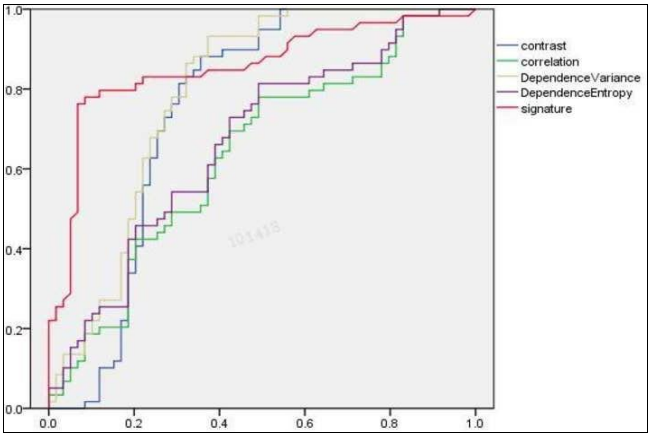

Fig 1: The AUC of contrast was 0.749. The AUC of correlation was 0.635. The AUC of Dependence Variance was 0.789. The AUC of Dependence Entropy was 0.666. The AUC of the model (signature) was 0.854

A logic regression model was established by using Contrast, Correlation, DependenceVariance, and DependenceEntropy. The coefficients were negative numbers for Contrast and DependenceVariance, while were positive numbers for Correlation and DependenceEntropy. The AUC of the regression model in the discrimination of CKD5 and CKD1 was 0.854, significantly higher than those of the original features (P<0.001). The sensitivity, specificity, and accuracy of the model in identifying CKD5 were 88% (53/60), 87% (52/60), and 88% (105/120), respectively.

Discussion

The current study investigated the feasibility of bone CT radiomics in identifying CKD5. The most important findings were as follows: 1) CKD5 and CKD1 bones differed in four radiomics features besides mean CT density; 2) CT radiomics model had 88% sensitivity and 87% specificity in identifying CKD5.

In renal failure cases, elevated blood phosphorus level, reduced blood calcium level and increased PTH secretion

caused parathyroid hyperplasia [22-23]. PTH acts on bone to release Ca2+ to restore blood calcium levels. When renal failure further develops, the compensatory function fails, the high blood phosphorus and low blood calcium persist, and PTH is also secreted in large quantities to continue to mobilize the release of bone calcium. Such a vicious cycle will eventually lead to fibrous osteoarthritis [24, 25].

The release of bone Ca2+ causes bone micro-structure to change. Bone salt deposition disorder in CKD also influences the structure and strength of bone. It is well established bone salt deposition disorder and Ca2+ release is more serious in CKD5 versus CKD1. The bone CT density is expected to be lower in CKD5 than in CKD1. However, in this study, the CT density difference of CKD5 and CKD1 did not reach statistical significance. Thus, bone CT density is not feasible in the discrimination of CKD5 and CKD1.

Because of fibrous osteoarthritis and other ill conditions, the micro-structure of CKD bones is different from that of normal bones [26]. Fibrous osteoarthritis is more serious in CKD5 versus CKD1. Thus, CKD1 and CKD5 bones may differ in the microstructure. In recent years, CT radiomics provided a non-invasive way to study the microstructure of tissue [27]. The study tried to find the micro-structure difference of CKD1 and CKD5 bones by using CT radiomics. CKD1 and CKD5 bones actually differed in some radiomics features, which might correlate with bone structure. In the study, we established a logic regression model for improving diagnostic accuracy. The AUC, sensitivity, specificity and accuracy of the model were all above 0.8, significantly higher than any single feature. Thus, the model is more feasible in identifying CKD5.

The study has some limitations. First, invasive bone biopsy pathology was not used as the reference standard in detecting micro-structure change in CKD. As the L1 vertebra was deep in the body, a bone biopsy is not allowed by the ethics. Second, CT radiomics was only applied to the L1 vertebra, but not to other vertebrae or other bones. In a further study, we should obtain radiomics features of other vertebrae. Third, this is a single-center study with moderate size. Multi-center large-size studies are required to validate our results. We at least introduce a new way to discriminate CKD5 from CKD1.

In conclusion, bone CT radiomics is feasible in identifying CKD5.

Funding

This study has received funding by National Natural Scientific foundation of China (Number: 31630025, and 81571643).

Table 2: Abbreviation List

Chronic kidney disease	CKD
Renal Osteodystrophy	ROD
Bone mineral density	BMD
Glomerular Filtration Rate	GFR
Receiver Operator Characteristic	ROC
Area Under the Curve	AUC

References

1. Franco Palacios CR, Hoxhaj R, Goyal P. Chronic kidney disease recognition amongst physicians and advanced practice providers. Ren Fail. 2021; 43:1276-1280.
2. Ma H, Ouyang C, Huang Y, Xing C, *et al*. Comparison of microwave ablation treatments in patients with renal secondary and primary hyperparathyroidism. Ren Fail. 2020; 42:66-76.
3. Haarhaus M, Evenepoel P, European Renal Osteodystrophy (EUROD) workgroup, *et al*. Differentiating the causes of adynamic bone in advanced chronic kidney disease informs osteoporosis treatment. Kidney Int. 2021; 100:546-558.
4. Ott SM. Renal Osteodystrophy-Time for Common Nomenclature. Curr Osteoporos Rep. 2017; 15:187-193.
5. Pazianas M, Miller PD. Osteoporosis and Chronic Kidney Disease-Mineral and Bone Disorder (CKD-MBD): Back to Basics. Am J Kidney Dis. 2021; 78:582-589.
6. Bover J, Bailone L, López-Báez V, *et al*. Osteoporosis, bone mineral density and CKD-MBD: Treatment considerations. J Nephrol. 2017; 30:677-687.
7. Nitta K, Yajima A, Tsuchiya K. Management of Osteoporosis in Chronic Kidney Disease. Intern Med. 2017; 56:3271-3276.
8. Flythe JE, Assimon MM, Tugman MJ, *et al*. Characteristics and Outcomes of Individuals with Pre-existing Kidney Disease and COVID-19 Admitted to Intensive Care Units in the United States. Am J Kidney Dis. 2021; 77:190-203.
9. McCollough CH, Leng S, Yu L, *et al*. Dual- and Multi-Energy CT: Principles, Technical Approaches, and Clinical Applications. Radiology. 2015; 276:637-653.
10. Sutherland-Smith J, Hutchinson D, Freeman LM. Comparison of computed tomographic attenuation values for epaxial muscles in old and young dogs. Am J Vet Res. 2019; 80:174-177.
11. Zhu Y, Triphuridet N, Yip R, *et al*. Opportunistic CT screening of osteoporosis on thoracic and lumbar spine: A meta-analysis. Clin Imaging. 2021; 80:382-390.
12. Pickhardt PJ, Pooler BD, Lauder T, *et al*. Opportunistic screening for osteoporosis using abdominal computed tomography scans obtained for other indications. Ann Intern Med. 2013; 158:588-595.
13. Bhandari A, Ibrahim M, Sharma C, *et al*. CT-based radiomics for differentiating renal tumours: A systematic review. Abdom Radiol. 2021; 46:2052-2063.
14. Shi L, Zhao J, Peng X, *et al*. CT-based radiomics for differentiating invasive adenocarcinomas from indolent lung adenocarcinomas appearing as ground-glass nodules: Asystematic review. Eur J Radiol. 2021; 144:p109956.
15. Sun W, Liu S, Guo J, *et al*. A CT-based radiomics nomogram for distinguishing between benign and malignant bone tumours. Cancer Imaging. 2021; 21:p20.
16. Bi L, Liu Y, Xu J, *et al*. A CT-Based Radiomics Nomogram for Preoperative Prediction of Lymph Node Metastasis in Periampullary Carcinomas. Front Oncol. 2021; 11:p632176.
17. Yao X, Mao L, Lv S, *et al*. CT radiomics features as a diagnostic tool for classifying basal ganglia infarction onset time. J Neurol Sci. 2020; 412:p116730.
18. Zhang Y, Zhang B, Liang F, *et al*. Radiomics features on non-contrast-enhanced CT scan can precisely classify AVM-related hematomas from other spontaneous intraparenchymal hematoma types. Eur Radiol. 2019; 29:2157-2165.
19. Liu J, Lian T, Chen H, *et al*. Pretreatment Prediction of

Relapse Risk in Patients with Osteosarcoma Using Radiomics Nomogram Based on CT: A Retrospective Multicenter Study. Biomed Res Int. 2021; 2021:6674471.
20. Lin P, Yang PF, Chen S, *et al*. A Delta-radiomics model for preoperative evaluation of Neoadjuvant chemotherapy response in high-grade osteosarcoma. Cancer Imaging. 2020; 20:p7.
21. Acar E, Leblebici A, Ellidokuz BE, *et al*. Machine learning for differentiating metastatic and completely responded sclerotic bone lesion in prostate cancer: A retrospective radiomics study. Br J Radiol. 2019; 92:p20190286.
22. Zhao S, Gan W, Xie W, *et al*. A single-center experience of parathyroidectomy in 1500 cases for secondary hyperparathyroidism: A retrospective study. Ren Fail. 2022; 44:23-29.
23. Kritmetapak K, Kongpetch S, Chotmongkol W, *et al*. Incidence of and risk factors for post-parathyroidectomy hungry bone syndrome in patients with secondary hyperparathyroidism. Ren Fail. 2020; 42:1118-1126.
24. Casey KM, Karanewsky CJ, Pendleton JL, *et al*. Fibrous Osteodystrophy, Chronic Renal Disease, and Uterine Adenocarcinoma in Aged Gray Mouse Lemurs (Microcebus murinus). Comp Med. 2021; 71:256-266.
25. Li T, Wilcox CS, Lipkowitz MS, *et al*. Rationale and Strategies for Preserving Residual Kidney Function in Dialysis Patients. Am J Nephrol. 2019; 50:411-421.
26. Fujita R, Ota M, Sato D, *et al*. Comparison of the Efficacy and Renal Safety of Bisphosphonate Between Low-Dose/High-Frequency and High-Dose/Low-Frequency Regimens in a Late-Stage Chronic Kidney Disease Rat Model. Calcif Tissue Int. 2020; 107:389-402.
27. Lim HK, Ha HI, Park SY, *et al*. Prediction of femoral osteoporosis using machine-learning analysis with radiomics features and abdomen-pelvic CT: A retrospective single center preliminary study. PLoS One. 2021; 16:e0247330.